



# Storage of High-Strength Steel Flux-Cored Welding Wires in Urbanized Areas

Adrian Wolski<sup>1</sup> · Aleksandra Świerczyńska<sup>1</sup> · Grzegorz Lentka<sup>2</sup> · Dariusz Fydrych<sup>1</sup>

Received: 3 March 2023 / Revised: 27 May 2023 / Accepted: 2 June 2023 / Published online: 17 June 2023  
© The Author(s) 2023

## Abstract

The condition of the consumables is a key factor determining the waste reduction in the welding processes and the quality of the welded joint. The paper presents the results of tests of four types of flux-cored wires dedicated for welding high-strength steels, stored for 1 month and 6 months in Poland in two urbanized areas: in a large seaside city (Gdańsk) and in Warsaw, located in the center of the country. The wires were subjected to macroscopic and microscopic (stereoscopic, SEM) observations, EDS analysis, technological tests assessing elastic properties and targetability. The degree of degradation of the wires was also tested using resistance measurements. In order to assess the effect of storing wires on the weldability of steel, the diffusible hydrogen content in deposited metal was determined by high-temperature extraction. It was found that the storage caused changes in the surface condition of the wires, affected their elasticity and electrical properties, which affects the behavior of the wires during welding. A significant influence of storage conditions on the hydrogenation of deposited metal was found: in the case of three types of wires, the level of low hydrogen processes was exceeded and the maximum result was 15.18 ml/100 g of deposited metal. It was also found that copper-plated wire showed a significantly increased resistance to storage conditions compared to non-copper-plated wires.

**Keywords** Arc welding · Flux-cored wire · Storage conditions · Weldability · Diffusible hydrogen content

## 1 Introduction

Among the various manufacturing processes, welding is a worldwide popular metal joining method that uses consumables as an essential material [1, 2]. Unfortunately, very often in industrial conditions consumables are subject to degradation, wear, destruction or deprivation of their properties due to improper storage. Such an unsustainable company policy generates direct losses—the waste of materials, as well as increased energy consuming and production costs—repair of defects, failures.

The quality of welded joints is the result of many factors occurring before, during and after the welding process [3, 4]. One of these factors is the condition of welding consumables: covered electrodes, fluxes, welding rods and wires, as well as shielding gases [5–8]. Reputable producers of consumables ensure proper transport and storage conditions for their products and recommend rules for storing them in production conditions. According to the guidelines of the standards regulating the quality requirements for the welding of metallic materials (e.g. ISO 3834-2 standard), manufacturers of welded structures should store consumables in warehouses with controlled and regulated conditions: temperature and relative humidity [9]. The ranges of recommended conditions are strictly defined and matched to the products of a given manufacturer. This is particularly evident for flux-cored wires, which (next to covered electrodes) are considered to be extremely sensitive to environment [10–12]. For most grades of flux-cored wires, the maximum temperature should not exceed 30 °C, and the relative humidity should not be higher than 80% [13]. However, the flux-cored arc welding (FCAW) process is used in transport, energy, mining, offshore,

✉ Aleksandra Świerczyńska  
aleksandra.swierczynska@pg.edu.pl

<sup>1</sup> Institute of Manufacturing and Materials Technology, Faculty of Mechanical Engineering and Ship Technology, Gdańsk University of Technology, Gabriela Narutowicza Street 11/12, 80-233 Gdańsk, Poland

<sup>2</sup> Department of Metrology and Optoelectronics, Faculty of Electronics, Telecommunications and Informatics, Gdańsk University of Technology, Gabriela Narutowicza Street 11/12, 80-233 Gdańsk, Poland

construction, in various climatic and hydrometeorological zones, with varying degrees of industrialization, which does not always make it possible to maintain appropriate storage conditions [14–16]. The consumable in the FCAW method is flux-cored wire with a ceramic or metal core (flux) and an outer, metal tube (sheath). Flux-cored wires can be divided to filled with rutile, basic or metal fluxes, to copper-plated or non-copper-plated wires or to seamed or seamless wires. The complex structure of flux-cored wires and their production process are determinants of particular susceptibility to unfavorable phenomena: changes in properties, occurrence of various types of corrosion and increased diffusible hydrogen content in deposited metal [13, 17, 18]. The latter factor, together with residual stress and brittle microstructure, is the reason for the formation of cold cracks [19–22].

The analysis of the literature shows that the moisture absorption by wires depends on the method of wire production, its construction and storage conditions. First of all, it is commonly believed that seamless wires are less susceptible to moisture penetration into the interior (flux) [23]. It should be emphasized that wire manufacturers very rarely recommend drying them to remove moisture, which is a standard technological procedure in the case of covered electrodes [24, 25]. For this reason, more attention should be paid to preventing the moisture pick up.

Although FCAW is a process that increases the share in the welding market, the lack of information about the influence of the environment on the condition of wires and the suitability for use resulting from potential changes in their condition is clearly noticeable. The literature review shows that the most complete research in this area was presented by Harwig et al. [26]. In this work, wires made of mild and Cr–Mo steel grades stored for 1 week in a climatic chamber (RH=80%, T=27 °C) and in atmospheric conditions were examined, and it was found that the tendency to hydrogenate the deposited metal strongly depends on the grade and type of wire. The results of research on the plasticity of bead-on-plate welds made using two types of seamless, copper-plated, flux-cored wires for non-alloy steel welding stored in two locations are presented in article [24]. The test results show that changes in storage conditions strongly affect the quality of welding wires and the mechanical properties of the welded joints made with them. Similar conclusions were drawn based on the research described in [13].

More attention was given to the study of the influence of welding parameters on diffusible hydrogen content in deposited metal obtained with FCAW process [17]. Other research trends involving FCAW welding include: fatigue and wear testing of the joints [27–30], development of flux-cored wires for underwater applications and welding of dissimilar joints [31–33] as well as applications for hybrid and additive processes [34].

The aim of this work is to present the effects of the environmental, urban conditions on changes in technological features, properties and quality of flux-cored wires for welding high-strength steels. To the best of the authors' knowledge, the presented research results are the first attempt in terms of this aspect of technological weldability of steel grades with yield strength above 460 MPa.

## 2 Materials and Methods

Four grades of flux-cored wires with a diameter of 1.2 mm and a weight of 5 kg from different manufacturers were used in the tests. Welding of high-strength steel was carried out with the use of the 136 method (FCAW-G according to ISO 4063). The wires have been marked for unambiguous identification: A, B, C and D. Below are their designations according to ISO 17632, where:

- A wire: T 55 4 Z P M21 H5;
- B wire: T 69 4 ZMn2.5NiMo P M21 2 H5;
- C wire: T 55 5 Mn1Ni P M 2 H5;
- D wire: T 62 5 MnNiMo P M 2 H5.

All of the tested wires have a flux, rutile core. B wire is a seamless wire and is covered with a layer of copper. A, C and D wires are coiled (seamed) and non-copper-plated. Tables 1 and 2 show the chemical composition of each wire grade and the mechanical properties of the weld metal.

Spools of wire without the packaging were stored in two locations in Poland: Gdańsk, in an urbanized area near the shipyard (54° 22' 43.684" N 18° 37' 51.548" E); Warsaw, in a highly urbanized area in the city center (52° 12' 15.723" N 21° 0' 1.465" E). The exposure period lasted a month (from January 4 to February 4) and half a year (from January 4 to July 4). The wires were stored in real conditions, in specially designed test stands, protecting wires against

**Table 1** Chemical composition of the weld metal of the tested flux-cored wires (according to manufacturer's certificates)

Wire grade	C [%]	Si [%]	Mn [%]	P [%]	S [%]	Cu [%]	Ni [%]	Mo [%]	Ti [%]	B [%]
A	0.05	0.37	1.25	–	–	–	0.93	0.12	–	–
B	0.06	0.46	1.82	0.012	0.005	0.22	2.19	–	–	–
C	0.05	0.33	1.51	0.009	0.008	–	0.95	0.16	0.055	0.0037
D	0.05	0.36	1.90	0.008	0.011	–	0.97	0.46	–	–

**Table 2** Mechanical properties of the weld metal of the tested flux-cored wires (according to manufacturer's certificates)

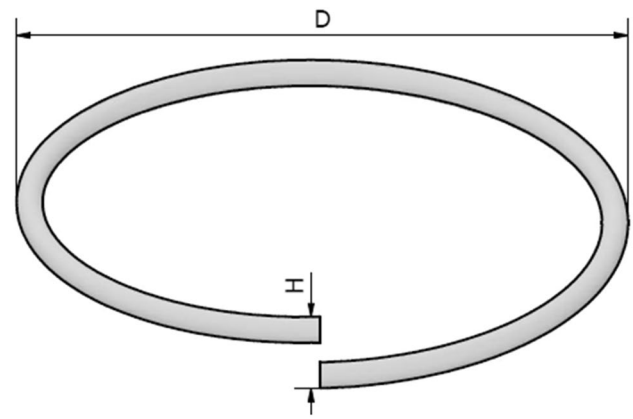
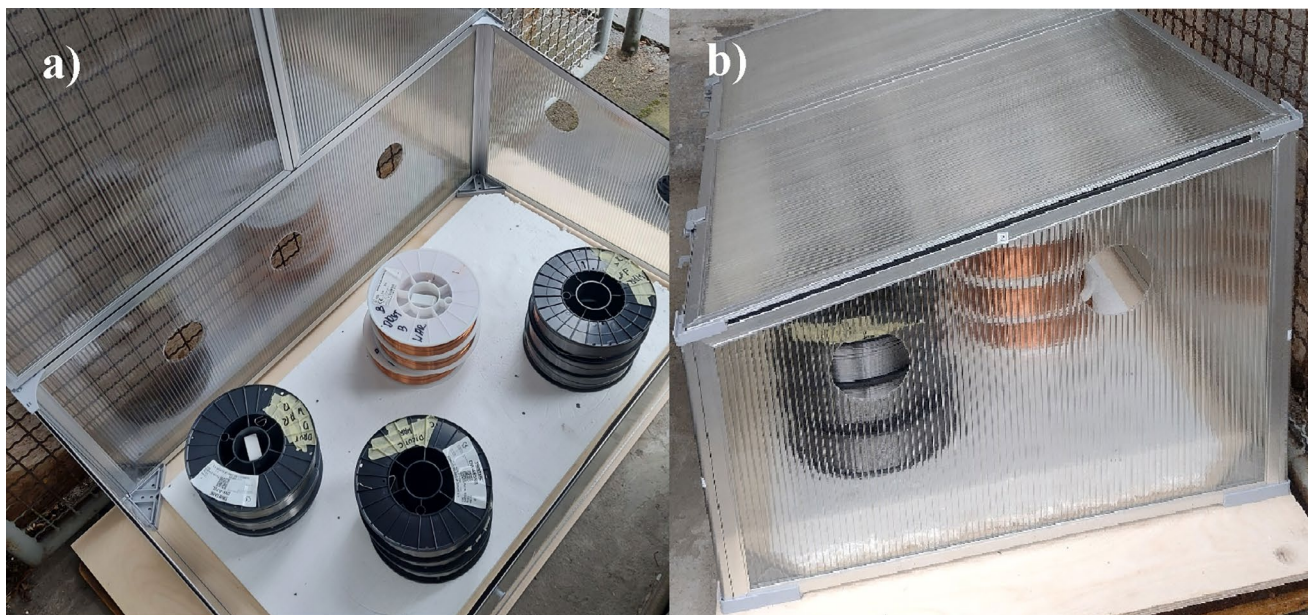
Wire grade	Tensile strength [MPa]	Yield strength [MPa]	Elongation [%]
A	640–790	Min. 550	20
B	770–900	Min. 690	Min. 17
C	640–760	Min. 550	Min. 18
D	700–890	Min. 620	Min 18

atmospheric precipitation, but allowing free air circulation. Figure 1 shows photographs of the test stand during storage of wires. During storage, temperature and relative humidity were measured and recorded every 30 min. For this purpose, the Termioplus recorder with the SHT15 sensor was used (temperature recording with a resolution of 0.1 °C, humidity recording with a resolution of 0.1% RH). Reference wire spools was stored in a sealed, closed package in a warehouse with appropriate humidity and temperature conditions. For the purposes of this article, the following wire designations have been adopted: first letter means the grade of the wire, second letter is connected to location: G for Gdańsk and W for Warsaw and the number at the end indicates the storage time (1 per 1 month, 6 per 6 months).

After the storage period, the outer surface of the wires was visually inspected. For each of the wires, a series of images was taken at 1× and 2× magnification. In addition, microscopic observations were carried out using a Delta Optical DO SZ-430 T stereoscopic microscope. Surface

observations and chemical composition analysis were also carried out using scanning electron microscopy (SEM–EDS, Phenom ProX Desktop SEM, Phenom World (Waltham, MA, USA)).

Technological tests of the quality of wires were carried out in accordance with the ISO 544:2018-02 standard: tests of wire unwinding and helical lift. These tests consist in cutting out one circle of the welding wire and placing it freely on a flat surface. Then, the measurement of the quantities marked in Fig. 2 was performed. The average values of five measurements were taken as the result. The standard does not provide guidelines for flux-cored wires, therefore the criteria applicable to solid wires were used in current tests. The

**Fig. 2** Scheme of measurement of the helical lift—H and the unwinding of the wire—D**Fig. 1** Test stand for storing wires in Warsaw **a** top view of the test stand interior and tested wires; **b** side view during the storage process (closed cover)

tested flux-cored wires were wound on spools with an outer diameter of 200 mm. For this diameter, the helical lift should not exceed 25 mm. Considering the wire unwinding, the PN-EN ISO 544:2018-02 standard does not contain guidelines as to the values that should be reached. There is only a recommendation that the wire unwinding, helical lift and surface condition of the wires should allow even, uninterrupted feeding on automatic or semi-mechanical equipment. For this reason, the unwinding test results were interpreted using the comparative method.

Another technological test—targetability measurement was carried out on a dedicated test stand. The scheme of conducting the test and taking measurements is shown in Fig. 3. The MIG 180 degree 5 m Master welding machine gun was placed on the trolley in such a way, that the CTWD was 150 mm. The consumable was extended to a distance of CTWD and the point of contact with the plane was marked. In this way, a series of five measurements was made for each wire. For the obtained measurement points, the diameter ( $d$ ) of the circle circumscribed on these points and the distance ( $R$ ) of the center of the circle from the "0" point (which is potentially determined with a perfectly straight wire) were determined. Diameter  $d$  is a measure allowing to assess the precision (repeatability) of the wire feeding, while the measure  $R$  indicates the accuracy of the wire feeding. Targetability test of welding wire feed is not standardized, so own criteria have been adopted. The criterion for evaluating targetability tests is that the wire should have the best possible concentration of wire feed measurement points during the tests described by the diameter " $d$ ". Ideal targetability would give parameters equal to  $R=0$  and  $d=0$ . In real conditions it is impossible to obtain. However, in the case of automated welding, obtaining a stable value of these parameters, even far from zero, will allow for a stable welding process.

In order to assess the degree of changes occurring in the wires, a test stand for measuring the resistance of wires was designed and built. A modified technical method was used for the resistance measurement. The measurement system (Fig. 4) uses a current source as the measurement excitation (current measurement takes place inside the device). The measuring current (with a value depending on the resistance measurement range) flows out from the I+ terminal, flows through a serial connection of the wire sections—the measured section and the reference section and then returns to the measuring device via the I- terminal. Differential inputs U1+, U1- and Uref+, Uref- are used to measure the differential voltage drop on the wire sections caused by the test current flow. The values of voltage drop U1 and Uref as well as the value of the measuring current allow to determine the resistance values of both sections of the wire.

Low values of the measured resistances (of the order of  $m\Omega$ )—comparable to the resistance of the connecting wires, make it necessary to use 4-terminal connections (Kelvin terminals), as shown in Fig. 4. Another important aspect is the need to compensate the influence of temperature. Resistance changes caused by temperature changes (even relatively small ones, of the order of a few  $^{\circ}\text{C}$ ) can be greater than changes in resistance caused by corrosion changes. Hence, the measurement using two sections of the wire—the measured and the reference, i.e. in the delivery state—assuming that both are at the same temperature and by determining the ratio of these resistances, the undesirable influence of temperature can be eliminated. The resistance values also depend on the length of the wire section, it is crucial in the measurement to ensure the stability of the length of the measured and reference wire sections—this is ensured by the measuring head. A series of at least ten measurements was made for each wire. The results were presented in the

**Fig. 3** Scheme of the targetability test **a** scheme of test stand, where: 1: welding gun, 2: flux-cored wire, 3: measurement plane, 4: measurement point; **b** method of taking measurements

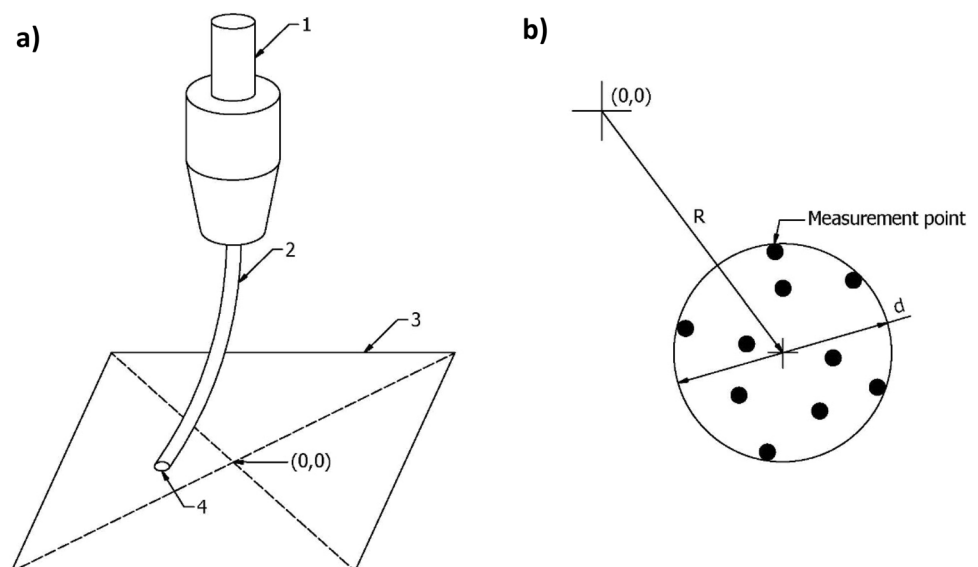
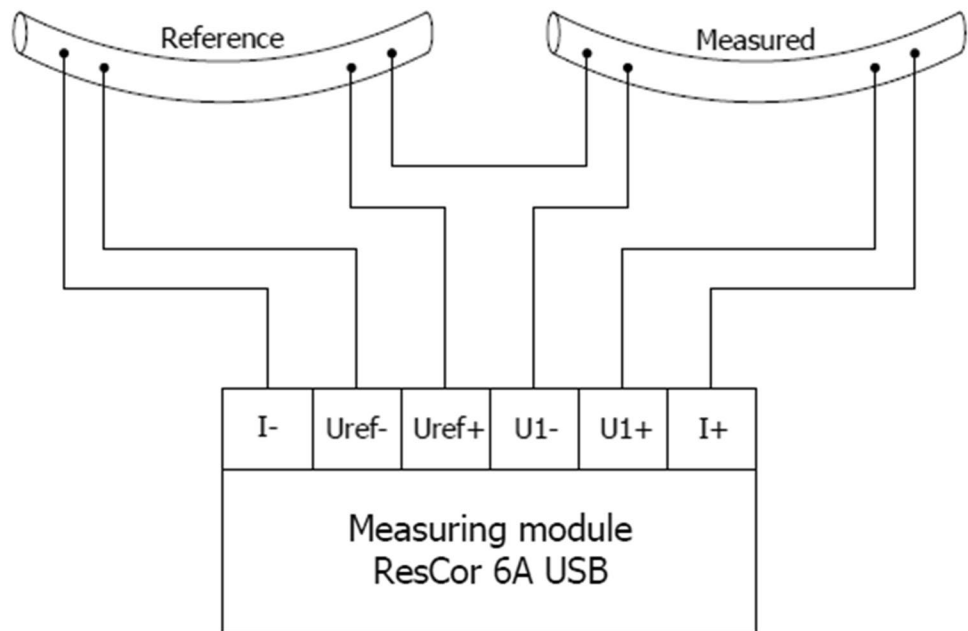




**Fig. 4** Scheme of the test stand for testing the resistance coefficient of stored wires with the method of connecting the tested wires



form of the resistance coefficient—ratio of measured and reference resistances.

Measurements of the diffusible hydrogen content in deposited metal were made by high-temperature extraction method using a Bruker G4 Phoenix device equipped with a thermal conductivity detector. Standard specimens were used for the tests as for the mercury method, in accordance with ISO 3690 [35, 36]. Before welding the specimens were weighed with the accuracy of 0.01 g. Padding welds were made for all tested wires using the automated method, with a M21 (Ar + 18% CO<sub>2</sub>) shielding gas, with the same parameters: wire feed rate 7.8 m/min, arc voltage 25 V, welding speed 31.1 cm/min, CTWD 25 mm, shielding gas flow rate: 17 L/min. MIG 4004i Pulse welding source with Feed 3004 feeder and ESAB Miggytrac 1001 trolley were used. The specimen was placed in copper fixture and then weld bead was deposited. After completion of welding the slag was removed, the specimen was quenched in water at 20 °C and stored in liquid nitrogen vessel. Hydrogen extraction was carried out at 400 °C for 30 min. The results are given as average values of three specimens.

### 3 Results

#### 3.1 Urban Storage Conditions

Figures 5 and 6 show graphs of temperature and relative humidity changes during storage of wires in Gdańsk and Warsaw. In addition, horizontal lines for average values of temperature and relative humidity were drawn. The course of changes in atmospheric conditions is typical for the

temperate climate of Poland, with greater daily variability of the results of temperature and relative humidity measurements in Gdańsk. In the analyzed period of time, the temperature in Gdańsk at the test stand ranged from – 3.6 °C to 46.9 °C (average 10.5 °C), and relative humidity from 14.7 to 99.3% (average 64.0%). In the test stand in Warsaw, the temperature ranged from – 4.1 °C to 32.6 °C (average 12.4 °C) and air humidity from 30.9 to 98.4% (average 66.5%). Comparing these results with the manufacturers' guidelines, it appears that in each case both temperature and relative humidity exceeded the recommended values. For the wires used, the manufacturers' guidelines indicate that the relative humidity of the air should not exceed 40–80% for the temperature range of 5–30 °C (depending on the wire grade).

#### 3.2 Visual Testing

Observing the outer surfaces of the wires, it can be concluded that different grades degraded to a different extent in the same period and place of storage. Figures 7 and 8 show exemplary photographs of the outer surfaces of wires showing all possible levels of wire degradation (low, medium and high). In the case of A wire, after the first month of storage both in Gdańsk (Fig. 7a) and Warsaw, numerous corrosion centers were visible (wire from Warsaw was visually more degraded). After 6 months, A wire was corroded to a large extent, the most among all wire grades (Fig. 7b). B wire was characterized by a low degree of degradation (the lowest among all the grades used). After 1 month, no corrosion centers were visible macroscopically (Fig. 7c), after 6 months, single corrosion centers (both from Gdańsk and Warsaw) began to appear (Fig. 7d). On the other hand, C

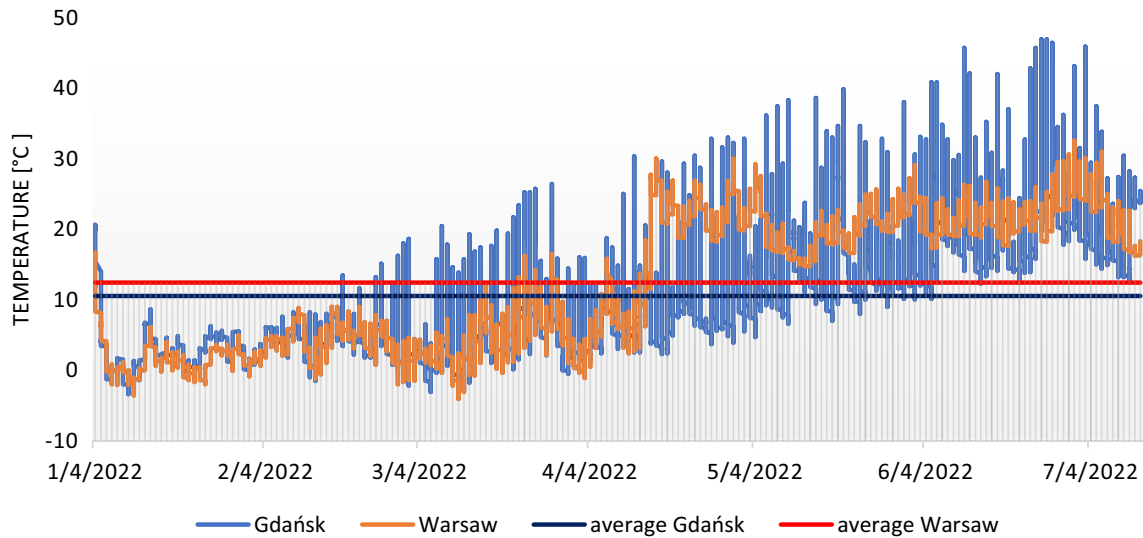


**Fig. 5** Changes in air temperature at test stands during storage of wires in Gdańsk and Warsaw

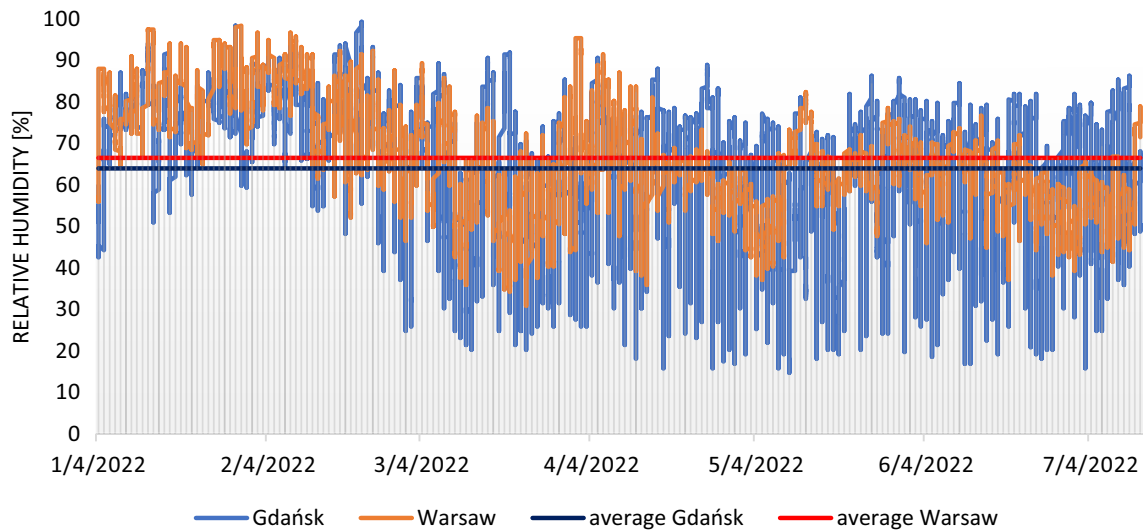


**Fig. 6** Changes in relative humidity at test stands during storage of wires in Gdańsk and Warsaw

and D wires after storage showed an average level of degradation, regardless of the storage location (Fig. 8). After a month, single, sporadic corrosion centers were visible on both wires (Fig. 8a, c). After half a year, the number of corrosion centers increased moderately (Fig. 8b, d), but not as much as in the case of A wire.

Microscopic examinations confirmed the results of visual observations. As can be seen from Fig. 9 showing representative wires, there was a significant increase in the number of changed areas on the surface of wires stored longer. After 1 month, A wire has numerous small corrosion precipitates on its surface (Fig. 9a), while after 6 months some of them merge and cover a larger area (Fig. 9b). On the

B wire, which had been in unfavorable conditions longer (Fig. 9d), local changes began to appear, probably indicating local condensation of water vapor, however, the wire stored for a shorter period showed no visible changes on the surface (Fig. 9c). A different mechanism of change can be seen on the C and D wires. In both cases, 1-month storage did not show large differences on their surface (Figs. 9e, g), but longer storage resulted in the appearance of large areas degraded by atmospheric corrosion occurring on them (Figs. 9f, h). These observations are consistent with the results of corrosion resistance tests of steel subjected to the impact of the urban environment reported by various authors [37–39].

**Fig. 7** Photographs of the outer surface of the wires after storage in Gdańsk **a** wire A, 1 month; **b** wire A, 6 months; **c** wire B, 1 month; **d** wire B, 6 months

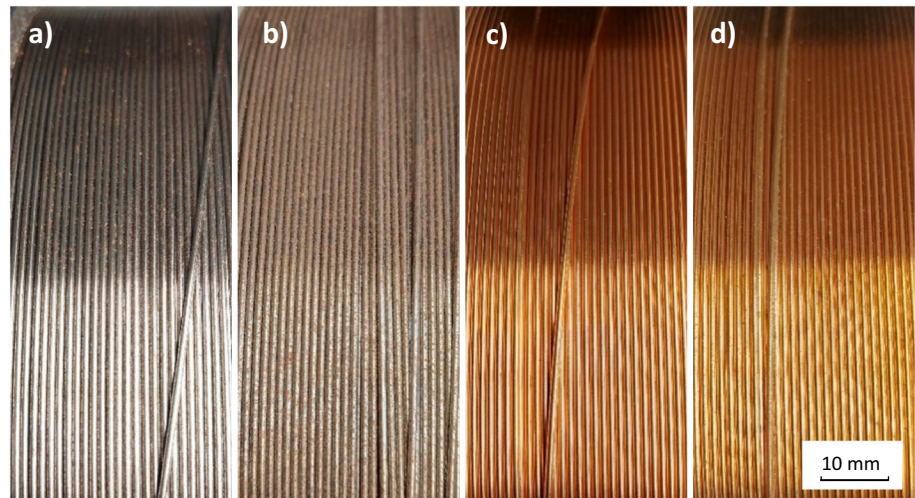


**Fig. 8** Photographs of the outer surface of the wires after storage in Warsaw **a** wire C, 1 month; **b** wire C, 6 months; **c** wire D, 1 month; **d** wire D, 6 months

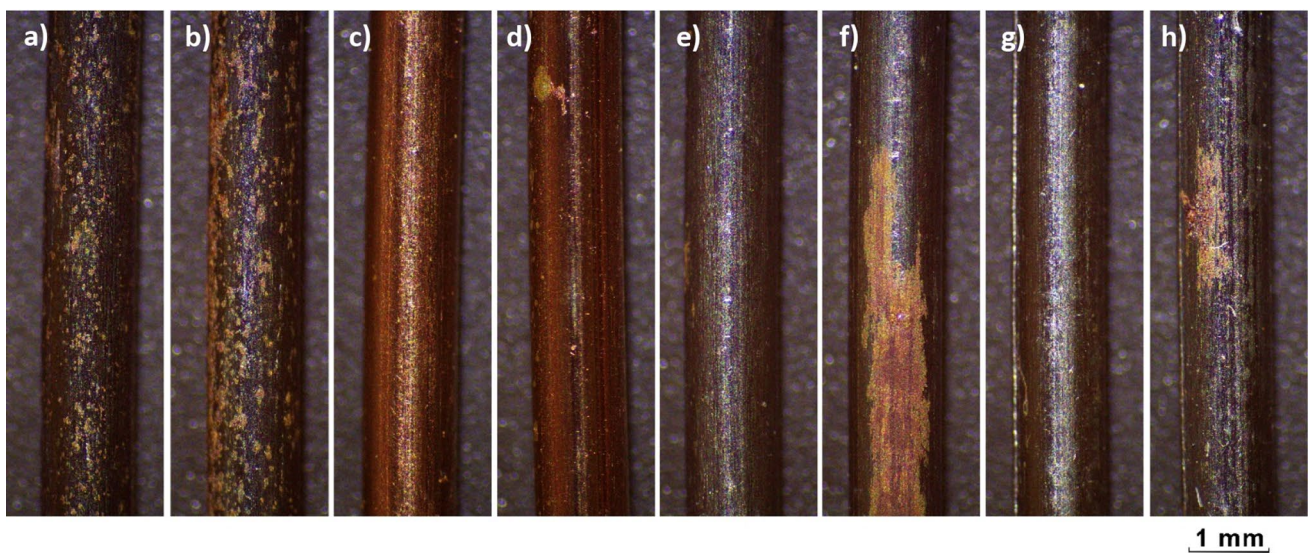
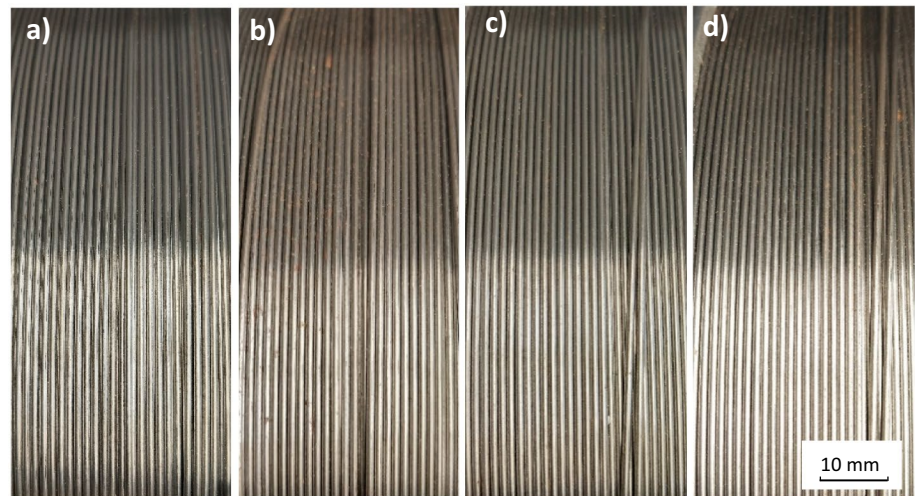


**Fig. 9** The surfaces of selected wires after storage; **a** wire A, Gdańsk, 1 month; **b** wire A, Gdańsk, 6 months; **c** wire B, Gdańsk, 1 month; **d** wire B, Gdańsk, 6 months; **e** wire C, Warsaw, 1 month; **f** wire C, Warsaw, 6 months; **g** wire D, Warsaw, 1 month; **h** wire D, Warsaw, 6 months



### 3.3 SEM Observations

Examples of SEM photographs of the selected wires are shown in Fig. 10. As can be seen in Fig. 10a, corrosion changes on the surface of A wire appeared in many areas of the wire. On the same grade of wire stored longer (Fig. 10b), these changes were more developed. The surface of these wires is also covered with streaks of lubricant from the manufacturing process of the wire. On the surface of B wire, the changes are slight, the surface is smooth both after 1 (Fig. 10c) and after 6 months (Fig. 10d). C and D wires showed similar degradation levels. In both cases, it was observed that large areas of the wire surface did not degrade in the form of precipitates appearing on them, but the wire surface itself degraded—it became cracked (Figs. 10e, f). Figure 10e also shows the longitudinal grooves on the wire, which were created during its drawing at the production stage.

The EDS analysis of the wire surface allowed to compare the chemical composition of the precipitates that appeared on the wires after storage in different locations. A characteristic feature of the wires stored in Gdańsk was the presence of sodium, which probably appeared as a result of the presence of sodium chloride in this seaside location. Figure 11a shows that in this case the precipitates are mainly iron oxides. Similarly, on the surface of C wire (Fig. 11b), iron oxide is the primary precipitate appearing on the surface. Among the elements detected there is also calcium, the presence of which may result from the release of ceramic powder components, probably through the seam. However, for the Warsaw location, no sodium appeared on any of the wires, even after prolonged storage.

### 3.4 Stiffness Tests

Tables 3 and 4 show the results of measuring helical lift (H) and wire unwinding (D). In order to analyze the values, reference was made to the PN-EN ISO 544:2018-02 standard. B and C wires meet the guidelines (max. 25 mm) at all times and in all storage locations. In addition, all the values of helical lifts for these wires are very close to each other. However, in A and D wires there is a large spread of helical lift results and there are specimens that exceed the value of 25 mm (A0, AG6, DG1, DW6). It can be seen that the main factor influencing the value of this parameter is the wire grade. Storing the wires causes changes in the helical lift in each of the wires. Analyzing the presented values of wire unwinding, it can be stated that for stored wires B, C and D they are similar. The maximum differences obtained for the given wires do not exceed 8.2 mm (maximum difference by the arithmetic mean: B = 1.2%; C = 2.0%; D = 1.7%). For each of these wires, the unwinding value for the reference wire is lower than that obtained

after storing the corresponding wire. The greatest dispersion of the results of wire unwinding was characteristic for A wire, where the maximum difference in the obtained results is 39.2 mm (maximum difference by the arithmetic mean: A = 9.0%). It is also noteworthy that with the increase in the storage time for A wire, there is both a downward and an upward trend in the value of wire unwinding (for Gdańsk, the value decreases, for Warsaw, it increases). D wire shows an upward trend and B wire a downward trend in wire unwinding with storage time.

### 3.5 Targetability Test

The results of the targetability test for reference and stored wires are shown in Table 5. B wire showed almost identical results for each storage time and location tested (11 and 12 mm), but higher than for the reference condition. Comparing these results with other wires, these values are higher than for C and D wires, which in several cases reached values of 8 and 9 mm. For C and D wires it is visible that the d values are similar after storing them and that these wires significantly differed in this parameter in the reference state. A wire is characterized by the greatest variability in terms of concentration of measurement points (d parameter). The best results (compared to all tested wires) were achieved after 1 month of storage in Gdańsk. After 1 month of storage in Warsaw, the obtained results were similar to reference wire. However, after 6 months of storage, the results of feeding precision were the worst of all wires (14 and 16 mm).

For all the tested wires, the R parameter did not show significant variability for stored wires, which justifies the conclusion that it is not a sufficiently sensitive indicator for assessing the elasticity and stiffness of the tested series of wires. On the other hand, all of the reference wires show a higher R parameter than their stored counterparts. For each of the wires, the storage increased the accuracy—the measurement points were closer to the "0,0" point (as in Fig. 3).

### 3.6 Electrical Resistance Measurements

The results of the wire resistance measurements are presented in Table 6. The values of the resistance coefficients indicate changes in the conductivity of the wires after the storage process. A coefficient above 1.00 indicates that the wire has a higher resistance than the reference (as delivered) wire. In most cases of wires (except AW and BG) the electrical resistance increased with storage time. For most wires stored for one month, the resistance coefficient is less than 1.00. For wires stored for six months, in most cases, the electrical resistance is higher than the reference wire (coefficient above 1.00). A wire had a lower electrical resistance than the reference wire in each case.



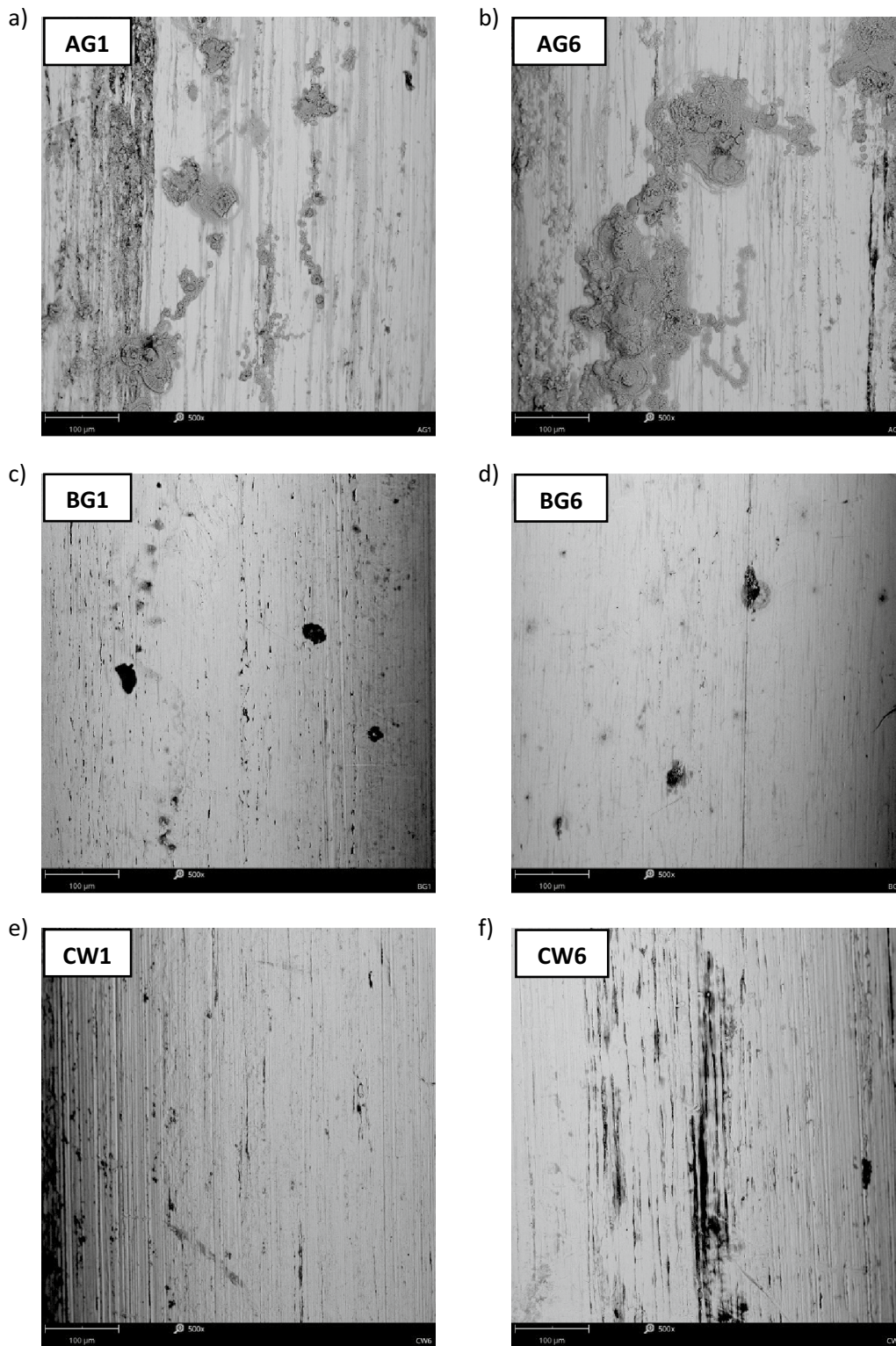
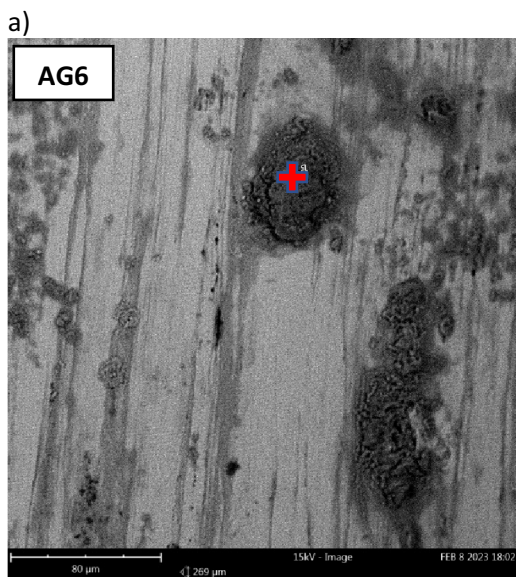
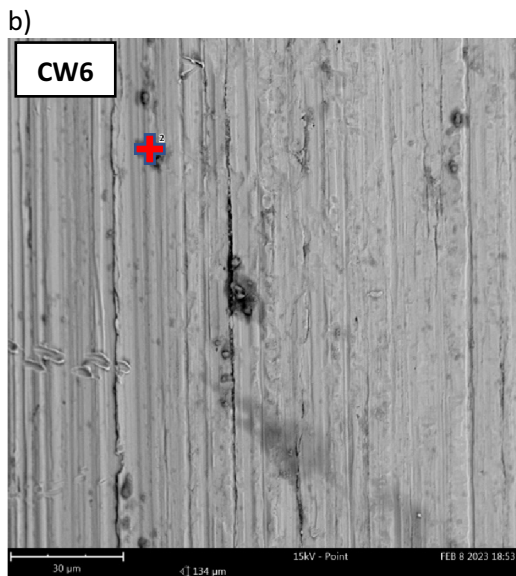


**Fig. 10** SEM images of the surface of selected wires after storage at 500× magnification: **a** wire A, Gdańsk, 1 month; **b** wire A, Gdańsk, 6 months; **c** wire B, Gdańsk, 1 month; **d** wire B, Gdańsk, 6 months; **e** wire C, Warsaw, 1 month; **f** wire C, Warsaw, 6 months



Element concentration (wt %), SEM-EDS					
O	Fe	N	C	Na	S
48.35	23.43	16.14	7.86	2.32	1.90



Element concentration (wt %), SEM-EDS				
Fe	O	N	Ca	S
72.56	18.97	6.41	0.93	0.81

**Fig. 11** SEM images of surface of the wires after storage at high magnification, and the results of chemical analysis via SEM-EDS; **a** wire A, Gdańsk, 6 months; **b** wire C, Warsaw, 6 months

**Table 3** Helical lift measurement results of reference and stored wires

Wire grade	Helical lift H [mm]				
	Reference wire	1 month		6 months	
		Gdańsk	Warsaw	Gdańsk	Warsaw
A	38.290	15.526	20.182	31.908	10.682
B	5.728	4.246	4.002	5.386	4.438
C	1.654	3.830	3.976	2.634	4.208
D	21.686	35.268	18.392	24.530	31.126

**Table 4** Wire unwinding measurement results of reference and stored wires

Wire grade	Wire unwinding D [mm]				
	Reference wire	1 month		6 months	
		Gdańsk	Warsaw	Gdańsk	Warsaw
A	434.4	440.2	436.4	411.0	450.2
B	340.4	348.6	345.2	341.0	344.2
C	403.0	414.0	406.2	414.4	410.6
D	379.8	389.4	388.2	394.6	395.0

**Table 5** Targetability measurement results of reference and stored wires

Wire grade	Reference wire		1 month				6 months			
			Gdańsk		Warsaw		Gdańsk		Warsaw	
	R [mm]	d [mm]	R [mm]	d [mm]	R [mm]	d [mm]	R [mm]	d [mm]	R [mm]	d [mm]
A	45	8	34	2	36	8	39	16	35	14
B	44	4	37	12	36	11	36	12	38	11
C	33	6	31	8	25	11	28	8	28	8
D	40	16	32	8	26	13	32	9	32	8

**Table 6** Stored wires resistance measurement results

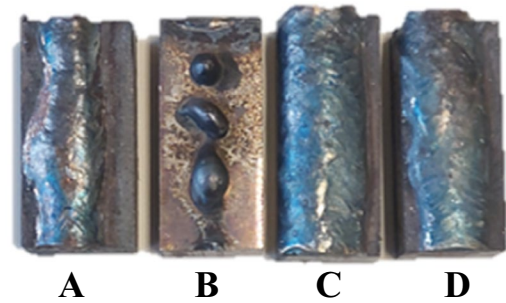
Specimens	Resistance coefficient value	
	1 month	6 months
AG/Ref	0.941828	0.944933
AW/Ref	0.986446	0.982623
BG/Ref	1.050438	0.987988
BW/Ref	0.995866	1.005455
CG/Ref	1.006218	1.015184
CW/Ref	0.996223	1.006561
DG/Ref	0.984295	1.000908
DW/Ref	0.987899	1.004667

**Table 7** Results of diffusible hydrogen content in deposited metal obtained from stored wires

Wire grade	Diffusible hydrogen content in deposited metal [ml/100gFe]			
	1 month		6 months	
	Gdańsk	Warsaw	Gdańsk	Warsaw
A	11.67	15.18	12.57	14.35
B	2.08	1.89	1.35	1.75
C	9.84	12.23	12.11	10.73
D	10.33	10.76	13.50	10.46

### 3.7 Diffusible Hydrogen Content Measurement

The results of diffusible hydrogen content in deposited metal measurements are presented in Table 7 and examples of specimens for each wire are shown in Fig. 12. B wire stored in Warsaw for 6 months caused problems in maintaining a stable welding process. In Fig. 12 an example of B wire specimen obtained during an unstable welding process is also shown. Such specimens were treated as outliers. It was not possible to weld with the assumed parameters, it was necessary to increase the CTWD and wire feed rate (wire melting was unstable). Despite these problems, B wire was found to meet the manufacturer's specifications (below 5 ml/100 g Fe) after storage at each location. The average diffusible hydrogen content for this wire after storage under

**Fig. 12** Examples of specimens for diffusible hydrogen content in deposited metal measurement by high-temperature extraction, wires stored in Warsaw for 6 months

each condition did not even exceed the H4 level (according to AWS standard). The results obtained for the remaining wires indicate an intense influence of the conditions on the hydrogen content, causing the H10 level to be exceeded and qualifying welding with these wires as high hydrogen process. In the case of A wire, on average, the highest amount of diffusible hydrogen was obtained. The Warsaw location achieved several ml/100 g higher results than the Gdańsk location in the same period of time. C and D wires showed similar levels of diffusible hydrogen content under the same conditions, all in the range of 9.8–13.5 ml/100 g, suggesting similar sensitivity to the considered environment. The differences in the results between the wires are strongly related to their construction—the B wire, seamless, copper plated showed greater resistance than the A, C and D wires, seamed and non-copper-plated.

## 4 Discussion

There are not many publications dealing with the subject of testing flux-cored wires stored in urbanized areas and their impact on the properties of wires. This publication presents some tests that allow to verify changes in wire properties that may be caused by the storage conditions. Four grades of rutile flux-cored wires for welding high-strength steel grades with yield strength above 460 MPa were tested.



Throughout the storage period of the wires, the parameters of air temperature and relative humidity were recorded using sensors. Obtained measurements indicated high relative humidity and considerable temperature fluctuations during storage. These values even exceeded the guidelines of manufacturers whose welding consumables have the least restrictive requirements for storage parameters (relative humidity exceeded 80% and temperature sometimes reached values below 0 °C and above 30 °C). Currently, there are no consumables that could be stored in such conditions and then used to weld responsible structures that carry significant loads. The actual, unfavorable storage conditions were the main reason for the changes observed in the tested wires.

The conditions that prevailed during storage directly affected the condition of the external surface of the flux-cored wires, which was shown in the visual tests. Corrosion centers appeared and propagated on each of the wires along with the time of storage. Corrosion on wires proceeded with different intensity, which could be caused by a different chemical composition of the flux-cored wires (the presence of elements that increase corrosion resistance), production method (the presence of a seam in the wires, drawing conditions), or the presence of copper plating on the surface of the wires. Considering the criterion of visual assessment, the copper-plated seamless B wire was the best. This method of production may have a positive effect on the quality of the wire, but it is associated with additional production costs that must be paid by the buyer of the consumable. On the other hand, as indicated in article [24], not all copper-plated wires behave the same. The article shows that different copper-plated wires stored under the same conditions can show very different corrosion intensity on the surface. This indicates that not only the presence of the coating is important here, but also the technology of its application.

SEM observations show that the tested wires are very different from each other. The surface of the A wire was subject to local, spot changes. Corrosion products, which in the case of a coastal location, also contained sodium, grew on the surface. B wire, also during high magnification observations, did not show any major changes on its surface after storage. Single, dark stains probably resulted from dust pollution present in both locations—these were urbanized areas. C and D wires were characterized by a different degradation mechanism. What appeared to be unaltered areas during visual observations turned out to be a mostly clean, but degraded areas. Numerous cracks appeared on the metal along the grooves from the drawing process, often filled with corrosion products. These results are in line with research reports on constructions operating in high humidity conditions [40–42].

Moisture of the wires may result in a change in the stiffness of the wires, which was demonstrated by testing the helical lift and unwinding of the wire. Unfortunately, there

are no guidelines for flux-cored wires, so the criteria for solid wires have been used. An example of using these guidelines is the article [43], in which the author stated that the materials he analyzed—G3Si1 and G4Si1 electrode wires—meet the criteria of the standard. It was noticed that the A wire, which showed the most visible surface degradation during storage, was also characterized by the greatest scatter of the results of both helical lift and unwinding of the wires. In the case of these tests, B and C wires proved to be the best, showing the smallest changes in the tested parameters. Comparing the results for reference wires it can be seen that the main factor influencing stiffness is the wire grade. On the other hand, storage in real conditions for each of the wires resulted in changes in stiffness of different intensity.

Degradation of the outer surface of the wires can cause unstable wire feeding into the weld groove. This was also mentioned by researchers examining aluminum wires for additive manufacturing purposes [44]. In the targetability tests for the used wires, differences in the feeding concentration of different types of wires that were stored for different periods of time and in different places were noted. In this case, B wire was the most stable, maintaining constant values in each case of storage. The best concentration values were obtained by C and D wire, despite the fact that as a reference wire they showed a large difference in the results of the d parameter. The least stable was A wire, which also underwent the greatest degradation of the surface. The degradation can be attributed to the feed stability of the wire. In addition, the use of wires with a damaged and corroded outer surface will cause faster wear of the contact tips and blocking of the steel spiral. This situation can lead to an increase in the field into which the wire can be fed, to an unstable, intermittent welding process and the occurrence of geometric welding imperfections and poor welding completion.

The results of technological research (Tables 3, 4, 5) were analyzed in the Statistica software. From a mathematical point of view, as shown in Table 8, there is no direct relationship between stiffness and target ability test results. Correlation coefficient values are lower than 0.328. However, from a substantive point of view, wires that exhibit less unwinding will also likely exhibit a greater R parameter. However, this is also affected by the fact that the wire passes through the

**Table 8** Correlation matrix for technological variables

Variables	R parameter	d parameter	Helical lift	Wire unwinding
R parameter	1.000	0.038	− 0.234	0.274
d parameter	0.038	1.000	− 0.182	0.101
Helical lift	− 0.234	− 0.182	1.000	0.328
Wire unwinding	0.274	0.101	0.328	1.000

rollers in the feeder, through the spiral and contact tip, so it can be deformed, which will change the targetability results.

Measurements of the relative resistance of the wire were made, which showed that the electrical properties of the wire change depending on where and for how long the wire is stored. At the beginning of the storage period, corrosion processes are localized on the surface of the wires and cause its diameter to decrease. It is less intensely visible for copper-plated wires. Further storage of the wires slows down the corrosion processes due to the formation of a barrier of corrosion products—the decrease in diameter and the increase in resistance is limited. The decrease in resistance found for some wires may be the result of the participation of corrosion products in the conduction of electricity. The analysis of the literature shows that electrical properties of the oxide layer on metals strongly depend on many factors, primarily the chemical composition, morphology and thickness of the layer, conditions of oxide formation, surface preparation [45–47]. Electrical conductivity of oxide layers can be semi-conductive (n-type and p-type) [48]. Wielant et al. [49] found that by changing the atmosphere oxide layers of different thicknesses, constitution and resistance can grow on steel.

The diffusible hydrogen content in deposited metal was determined. It has been shown that the seamless wire best protects the consumable against environmental conditions causing an increase in diffusible hydrogen content in deposited metal. For B wire, the value of diffusible hydrogen assumed by the manufacturer (H5) was not exceeded, regardless of the time and place of storage. In the remaining cases (A, C and D wires) the content significantly exceeded the values set by the manufacturer. Similar results can be found in article [24], in which the authors examined the impact of atmospheric exposure on the diffusible hydrogen content in the conditions of a climatic chamber. After 1 week at 27 °C and 80% relative humidity FCAW-G deposits have been shown to be susceptible to increased diffusible hydrogen levels after atmospheric exposure. The following were indicated as the most important factors contributing to this growth: electrode manufacturer, packaging method and storage time. This is consistent with the results presented in this article. Increase of diffusible hydrogen content in deposited metal could have been caused by damage to the surface layer, lack of protection of the hygroscopic flux core against moisture and presence of corrosion products on the wire surface. It is confirmed by the highest results obtained for the most degraded consumable (A wire). The cause of this increase can be both the penetration of moisture into the wire and the accumulation of moisture on the surface of wires that have undergone degradation. The surface developed due to corrosion changes is a source of potential hydrogen. This can cause welding imperfections such as weld porosity and unacceptable hydrogen embrittlement [50–52]. In addition,

as shown in [13, 24], the storage conditions of the wires also affect the mechanical properties of the deposited metal.

## 5 Conclusions

In this work, the effect of storage of flux-cored wires for welding high-strength non-alloy steels on their properties was investigated. For this purpose, four grades of flux-cored wires were stored in two urbanized areas (Warsaw and Gdańsk, Poland) for one month and six months. The following conclusions can be drawn from the presented research:

1. Conditions in industrial and urbanized areas usually exceed the permissible values of temperature and relative humidity imposed by manufacturers of consumables for the storage of their products.
2. Storage in conditions exceeding the manufacturer's approvals causes degradation of wires in the form of corrosion on their surface, the size and intensity of which may vary depending on their construction, coating, location and storage time.
3. Tests of helical lift and unwinding of the wire indicate a change in the stiffness of the wires with the time of storage, which may cause problems with the stability of wire feeding.
4. The wires that tend to have the most intense surface degradation have a problem with stable accuracy of the wire feeding into the weld groove—targetability. This may result in arc wandering if it is possible to strike it. Wires that exhibit greater resistance to external factors maintain constant stability of wire feed precision for a significant period of storage in adverse conditions.
5. The electrical resistance of the flux-cored wires is a variable that depends on the storage conditions and time. Due to the formation of oxide layers, which can work as semiconductors storage causes an increase in the resistance of the wires, which after some time stabilizes and for some wires it decreases again.
6. Seamless wire (B) show significant resistance to external factors and maintain the parameter of hydrogen content H5 in deposited metal for a longer time of storage in unfavorable conditions. Seamed wires (A, C, D), after a short time of storage in urbanized areas, absorb moisture, causing an increase in the diffusible hydrogen content in deposited metal as for medium and high hydrogen processes.

**Acknowledgements** Authors would like to thank Prof. Tomasz Chmielewski and MSc. Mateusz Majchrzak from Warsaw University of Technology for kind help in storing flux-cored wires, Dr. Mirosław Szala from Lublin University of Technology for valuable discussions as well as Piotr Wesołowski and Dariusz Karubin for technical assistance and support during the research.



**Author Contributions** AW: Methodology, Investigation, Resources, Data Curation, Writing—Original Draft, Writing—Review and Editing, Visualization; AŚ: Conceptualization, Methodology, Investigation, Resources, Data Curation, Writing—Original Draft, Writing—Review and Editing, Supervision, Funding acquisition; Grzegorz Lentka: Methodology, Software; DF: Conceptualization, Methodology, Writing—Review and Editing, Supervision. All authors read and agreed upon the final version of the manuscript.

**Funding** Financial support of these studies from Gdańsk University of Technology by the DEC-18/2021/IDUB/I.3.3 grant under the ARGENTUM TRIGGERING RESEARCH GRANTS—‘Excellence Initiative—Research University’ program is gratefully acknowledged.

**Data availability** The data that support the findings of this study are available on request from the corresponding author.

## Declarations

**Conflict of Interest** On behalf of all authors, the corresponding author states that there is no conflict of interest.

**Open Access** This article is licensed under a Creative Commons Attribution 4.0 International License, which permits use, sharing, adaptation, distribution and reproduction in any medium or format, as long as you give appropriate credit to the original author(s) and the source, provide a link to the Creative Commons licence, and indicate if changes were made. The images or other third party material in this article are included in the article's Creative Commons licence, unless indicated otherwise in a credit line to the material. If material is not included in the article's Creative Commons licence and your intended use is not permitted by statutory regulation or exceeds the permitted use, you will need to obtain permission directly from the copyright holder. To view a copy of this licence, visit <http://creativecommons.org/licenses/by/4.0/>.

## References

- Skowrońska, B., Szulc, J., Bober, M., Baranowski, M., & Chmielewski, T. (2022). Selected properties of RAMOR 500 steel welded joints by hybrid PTA-MAG. *Journal of Advanced Joining Processes*, 5, 100111.
- Sirohi, S., Kumar, A., Soni, S., Dak, G., Kumar, S., Świerczyńska, A., & Pandey, C. (2022). Influence of PWHT parameters on the mechanical properties and microstructural behavior of multi-pass GTAW joints of P92 steel. *Materials*, 15(12), 4045.
- Kim, H., Lee, G., Shin, S., Yoo, H., Cho, J., Han, S. W., & Kim, G. (2022). Strength prediction FEM model development of welded steel joint. *International Journal of Precision Engineering and Manufacturing*, 23(12), 1399–1409.
- Saad, M. H., Darras, B. M., & Nazzal, M. A. (2021). Evaluation of welding processes based on multi-dimensional sustainability assessment model. *International Journal of Precision Engineering and Manufacturing-Green Technology*, 8, 57–75.
- Sharma, L., Chhibber, R., Kumar, V., & Khan, W. N. (2022). Element transfer investigations on silica based Submerged Arc welding fluxes. *Silicon*, 15, 301–319.
- Varbai, B., & Májlinger, K. (2019). Physical and theoretical modeling of the nitrogen content of duplex stainless steel weld metal: shielding gas composition and heat input effects. *Metals*, 9(7), 762.
- Sirohi, S., Pandey, S. M., Świerczyńska, A., Rogalski, G., Kumar, N., Landowski, M., & Pandey, C. (2022). Microstructure and mechanical properties of combined GTAW and SMAW dissimilar welded joints between Inconel 718 and 304L austenitic stainless steel. *Metals*, 13(1), 14.
- Coetsee, T., & De Bruin, F. (2022). Modification of flux oxygen behaviour via Co-Cr-Al unconstrained metal powder additions in submerged arc welding: gas phase thermodynamics and 3D slag SEM evidence. *Processes*, 10(11), 2452.
- Tomków, J., Fydrych, D., Rogalski, G., & Łabanowski, J. (2019). Effect of the welding environment and storage time of electrodes on the diffusible hydrogen content in deposited metal. *Revista de Metalurgia*, 55(1), e140.
- Yoo, J., An, H., Lee, J., Yun, K. H., Saha, S. K., & Kang, N. (2023). Prediction on cold crack sensitivity using hydrogen embrittlement index measured from in situ slow-strain-rate testing for multipass flux-cored arc weld metals of shipbuilding and offshore steels. *Materials Characterization*, 197, 112637.
- Amaral, E. C., Jácome-Carrascal, J. L., Moreno-Urbe, A. M., & Bracarense, A. Q. (2021). Influence of the formulation of a flux-cored wire on the microstructure and hardness of welded metal. *Journal of Physics*, 2118(1), 012010.
- Kordi, H. A., Ghasempour-Mouziraji, M., & Hosseinzadeh, M. (2021). Metal transfer mapping for flux-cored arc welding process by using near-infrared filming. *Journal of Materials Engineering and Performance*, 30(4), 3079–3095.
- Świerczyńska, A. (2019). Effect of storage conditions of rutile flux cored welding wires on properties of welds. *Advances in Materials Science*, 19(4), 46–56.
- Trembach, B., Grin, A., Turchanin, M., Makarenko, N., Markov, O., & Trembach, I. (2021). Application of Taguchi method and ANOVA analysis for optimization of process parameters and exothermic addition (CuO-Al) introduction in the core filler during self-shielded flux-cored arc welding. *The International Journal of Advanced Manufacturing Technology*, 114(3), 1099–1118.
- Trinh, N. Q., Tashiro, S., Suga, T., Kakizaki, T., Yamazaki, K., Lersvanichkool, A., & Tanaka, M. (2022). Metal transfer behavior of metal-cored arc welding in pure argon shielding gas. *Metals*, 12(10), 1577.
- Park, H., Park, C., Lee, J., Nam, H., Moon, B., Moon, Y., & Kang, N. (2021). Microstructural aspects of hydrogen stress cracking in seawater for low carbon steel welds produced by flux-cored arc welding. *Materials Science and Engineering A*, 820, 141568.
- Fydrych, D., Świerczyńska, A., & Tomków, J. (2014). Diffusible hydrogen control in flux cored arc welding process. *Key Engineering Materials*, 597, 171–178.
- Das, S., Vora, J. J., Patel, V., Li, W., Andersson, J., Pimenov, D. Y., & Wojciechowski, S. (2021). Experimental Investigation on welding of 2.25 Cr-1.0 Mo steel with regulated metal deposition and GMAW technique incorporating metal-cored wires. *Journal of Materials Research and Technology*, 15, 1007–1016.
- Brätz, O., Klett, J., Wolf, T., Henkel, K. M., Maier, H. J., & Hasel, T. (2022). Induction heating in underwater wet welding—thermal input, microstructure and diffusible hydrogen content. *Materials*, 15(4), 1417.
- Wasim, M., Djukic, M. B., & Ngo, T. D. (2021). Influence of hydrogen-enhanced plasticity and decohesion mechanisms of hydrogen embrittlement on the fracture resistance of steel. *Engineering Failure Analysis*, 123, 105312.
- Wilhelm, E., Mente, T., & Rhode, M. (2021). Waiting time before NDT of welded offshore steel grades under consideration of delayed hydrogen-assisted cracking. *Welding in the World*, 65(5), 947–959.
- Nam, H., Yoo, J., Yun, K., Xian, G., Park, H., Kim, N., & Kang, N. (2021). Comprehensive analysis of cold-cracking ratio for flux-cored arc steel welds using Y-and y-grooves. *Materials*, 14(18), 5349.
- Trinh, N. Q., Tashiro, S., Suga, T., Kakizaki, T., Yamazaki, K., Morimoto, T., & Tanaka, M. (2022). Effect of flux ratio on droplet transfer behavior in metal-cored arc welding. *Metals*, 12(7), 1069.



24. Świerczyńska, A., & Landowski, M. (2020). Plasticity of bead-on-plate welds made with the use of stored flux-cored wires for offshore applications. *Materials*, *13*(17), 3888.
25. Guo, N., Zhang, X., Fu, Y., Luo, W., Chen, H., & He, J. L. (2023). A novel strategy to prevent hydrogen charging via spontaneously molten-slag-covering droplet transfer mode in underwater wet FCAW. *Materials and Design*, *226*, 111636.
26. Harwig, D. D., Longenecker, D. P., & Cruz, J. H. (1999). Effects of welding parameters and electrode atmospheric exposure on the diffusible hydrogen content of gas shielded flux cored arc welds. *Welding Journal*, *78*, 314-s.
27. da Silva, M. S., Souza, D., de Lima, E. H., Bianchi, K. E., & Vilarinho, L. O. (2020). Analysis of fatigue-related aspects of FCAW and GMAW butt-welded joints in a structural steel. *Journal of the Brazilian Society of Mechanical Sciences and Engineering*, *42*(1), 1–13.
28. de Sousa, J. M. S., Lobato, M. Q., Garcia, D. N., & Machado, P. C. (2021). Abrasion resistance of Fe–Cr–C coating deposited by FCAW welding process. *Wear*, *476*, 203688.
29. Mičian, M., Winczek, J., Harmaniak, R., Koňár, R., Gucwa, M., & Moravec, J. (2021). Physical simulation of individual heat-affected zones in S960MC steel. *Archives of Metallurgy and Materials*. <https://doi.org/10.24425/amm.2021.134762>
30. Samadi, F., Mourya, J., Wheatley, G., Khan, M. N., Nejad, R. M., Branco, R., & Macek, W. (2022). An investigation on residual stress and fatigue life assessment of T-shape welded joints. *Engineering Failure Analysis*, *141*, 106685.
31. Yang, J., Xu, S., Jia, C., Han, Y., Maksymov, S., & Wu, C. (2023). A novel 3D numerical model coupling droplet transfer and arc behaviors for underwater FCAW. *International Journal of Thermal Sciences*, *184*, 107906.
32. Liu, S., Ji, H., Zhao, W., Hu, C., Wang, J., Li, H., & Lei, Y. (2022). Evaluation of arc signals, microstructure and mechanical properties in ultrasonic-frequency pulse underwater wet welding process with Q345 steel. *Metals*, *12*(12), 2119.
33. Maurya, A. K., Pandey, C., & Chhibber, R. (2021). Dissimilar welding of duplex stainless steel with Ni alloys: A review. *International Journal of Pressure Vessels and Piping*, *192*, 104439.
34. Pańcikiewicz, K. (2021). Preliminary process and microstructure examination of flux-cored wire arc additive manufactured 18Ni-12Co-4Mo-Ti maraging steel. *Materials*, *14*(21), 6725.
35. Yoo, J., Kim, S., Jo, M. C., Kim, S., Oh, J., Kim, S. H., & Sohn, S. S. (2022). Effects of Al-Si coating structures on bendability and resistance to hydrogen embrittlement in 1.5-GPa-grade hot-press-forming steel. *Acta Materialia*, *225*, 117561.
36. Rhode, M., Schaupp, T., Muenster, C., Mente, T., Boellinghaus, T., & Kannengiesser, T. (2019). Hydrogen determination in welded specimens by carrier gas hot extraction—A review on the main parameters and their effects on hydrogen measurement. *Welding in the World*, *63*, 511–526.
37. Zhang, H., Xu, J., Guo, L., & Dong, H. (2023). Study on rust layers of carbon steel, weathering steel and alloy steel exposed to Shanghai atmosphere for three years. *Materials Today Communications*, *35*, 105520.
38. Królikowska, A., Komorowski, L., Kunce, I., Wojda, D., Zacharuk, K., Paszek, U., & Bilewska, K. (2021). Corrosion assessment of a weathering steel bridge structure after 30 years of service. *Materials*, *14*(14), 3788.
39. Rodríguez-Yáñez, J. E., Batlle, S. F., Sanabria-Chinchilla, J., & Rojas-Marín, J. F. (2023). Combined effect of the exposure angle and face orientation on the atmospheric corrosion behavior of low carbon steel. *Electrochimica Acta*, *439*, 141567.
40. Walczak, M., Szala, M., & Okuniewski, W. (2022). Assessment of corrosion resistance and hardness of shot peened X5CrNi18-10 steel. *Materials*, *15*(24), 9000.
41. Trzepieciński, T., Kubit, A., & Slota, J. (2022). Assessment of the tribological properties of the steel/polymer/steel sandwich material LITECOR. *Lubricants*, *10*(5), 99.
42. Szala, M., & Łukasik, D. (2018). Pitting corrosion of the resistance welding joints of stainless steel ventilation grille operated in swimming pool environment. *International Journal of Corrosion*, *2018*, 9408670.
43. Turyk, E. (2021). Quality criteria for G3Si1 and G4Si1 electrode wires. *Bulletin of the Institute of Welding*, *65*(3), 39–47.
44. Gu, J. L., Ding, J. L., Cong, B. Q., Bai, J., Gu, H. M., Williams, S. W., & Zhai, Y. C. (2015). The influence of wire properties on the quality and performance of wire+ arc additive manufactured aluminium parts. *Advanced Materials Research*, *1081*, 210.
45. Magrasó, A., Falk-Windisch, H., Froitzheim, J., Svensson, J. E., & Haugrud, R. (2015). Reduced long term electrical resistance in Ce/Co-coated ferritic stainless steel for solid oxide fuel cell metallic interconnects. *International Journal of Hydrogen Energy*, *40*(27), 8579–8585.
46. Guo, L. Q., Yang, B. J., Liang, D., & Qiao, L. J. (2015). Surface preparation effect on duplex stainless steel passive film electrical properties studied by in situ CSAFM. *Journal of Materials Research*, *30*(20), 3084–3092.
47. Örnek, C., Zhang, F., Larsson, A., Mansoor, M., Harlow, G. S., Kroll, R., Carlà, F., Hussain, H., Engelberg, D. L., Derin, B., & Pan, J. (2023). Understanding passive film degradation and its effect on hydrogen embrittlement of super duplex stainless steel – synchrotron X-ray and electrochemical measurements combined with CalPhaD and ab-initio computational studies. *Applied Surface Science*, *628*, 157364.
48. Rubben, T., Baert, K., Depover, T., Verbeken, K., Revilla, R. I., & De Graeve, I. (2022). Influence of thermal oxide layers on the hydrogen transport through the surface of SAE 1010 steel. *Journal of The Electrochemical Society*, *169*(11), 111503.
49. Wielant, J., Goossens, V., Hausbrand, R., & Terryn, H. (2007). Electronic properties of thermally formed thin iron oxide films. *Electrochimica Acta*, *52*(27), 7617–7625.
50. Fydrych, D., Raczko, P., Świerczyńska, A., Landowski, M., Wolski, A., & Rogalski, G. (2023). Effect of arc strikes on high strength low alloy steels welded by SMAW. *Advances in Science and Technology Research Journal*. <https://doi.org/10.12913/22998624/166061>.
51. Parshin, S. G., Levchenko, A. M., & Maystro, A. S. (2020). Metallurgical model of diffusible hydrogen and non-metallic slag inclusions in underwater wet welding of high-strength steel. *Metals*, *10*(11), 1498.
52. Kim, J. Y., Yoon, S. C., Kim, H. J., & Lee, M. G. (2023). Enhanced hydrogen delayed fracture of 1.5 GPa hot stamping steel sheet with sheared surface by double punching method. *International Journal of Precision Engineering and Manufacturing*, *24*(2), 173–186.

**Publisher's Note** Springer Nature remains neutral with regard to jurisdictional claims in published maps and institutional affiliations.



**Adrian Wolski** is a PhD student at the Institute of Manufacturing and Materials Technology, Gdańsk University of Technology, Poland. His research interests are friction stir welding, underwater welding, mechanical testing of materials.



**Grzegorz Lentka** is a Professor at the Department of Metrology and Optoelectronics, Gdańsk University of Technology, Poland. His research interests are focused on digital signal processing for metrology, impedance spectroscopy measurement methods for diagnostics of technical objects, design of measurement and diagnostic systems for electronic circuits and objects modeled by electrical circuits, systems on a chip, smart sensors, energy consumption estimation for low-power microcontroller based devices and energy harvesting circuits.



**Aleksandra Świerczyńska** is an Associate Professor at the Institute of Manufacturing and Materials Technology, Gdańsk University of Technology, Poland. Her research interests include flux cored arc welding, environmental degradation of welded joints and welding consumables, underwater welding, hydrogen. She is also the Associate Editor of the Advances in Materials Science journal.



**Dariusz Fydrych** is a Professor at the Institute of Manufacturing and Materials Technology, Gdańsk University of Technology, Poland. His research interests are weldability of metals, underwater welding, dissimilar welding, flux cored arc welding, friction stir welding, explosion welding, design of experiment, multidimensional modelling. He is also the Deputy Editor-in-Chief of the Advances in Materials Science journal.